Inherent Structure in Water

Frank H. Stillinger* and Thomas A. Weber

Bell Laboratories, Murray Hill, New Jersey 07974 *(Received: December 28, 1982)*

The statistical thermodynamics of water has been recast in a form which distinguishes two basic contributions, one of purely structural origin, and one due to anharmonic vibrations. The former involves the collection of potential energy minima ("inherent structures") while the latter concerns thermal motions away from these minima. Information about the inherent structures has been adduced from crystallography and from molecular dynamics simulation for a 250-molecule cluster with free surfaces. We concluded that near 0 °C the mean molar volume of relevant inherent structures contributing to the liquid phase increases as temperature decreases, and that this increase probably has a singularity at the supercooling limit due to cooperative aggregation of hydrogen-bond polyhedra. Approximately 85–90% of the latent heat of melting ice can be attributed to upward shift in potential energy of the inherent structures across the transition, the remainder to changing anharmonicity.

I. Introduction

Water displays a formidable array of unusual physical and chemical properties in its condensed phases.[1,2] Because this substance is molecularly complex it is not surprising that the history of attempts to explain these properties has involved more imagination than insight. At present, any new approach which lightens the conceptual burden carried by those seeking to understand water at the molecular level would be most welcome.

We explore in this paper the possibility that such an approach can be constructed along lines previously employed to study phase change in two dimensions.[3,4] The basic idea concerns separation of the problem into two parts. The first part involves identification of a discrete set of inherent structures, each of which corresponds to a local minimum in the potential energy function for the system. The second part examines the generally anharmonic vibrations that the system executes about those minima. In fact this separation can be carried out uniquely and precisely, and at least in the two-dimensional application leads to a novel theory of melting.[4] The procedure for constructing this separation and some general implications that follow therefrom are outlined in section II.

Section III takes up the problem of classifying inherent structures in water according to their energies, densities, and bonding patterns. The available experimental data are surveyed and lead to some useful insights, but they are incapable of providing a complete picture. Consequently we turn in section IV to molecular dynamics computer simulation as an alternative source of information and report new results for a 250-molecule study.

Some of the well-known liquid water anomalies receive scrutiny in section V, specifically the density maximum phenomenon and the supercooling behavior. The use of the inherent structure viewpoint seems to offer conceptual advantages in classifying and unifying these anomalies.

We end our exposition with a few concluding remarks in section VI.

II. Statistical Mechanical Background

An obvious starting point for application of the inherent structure formalism to water is the canonical partition function:

$$Q_N(\beta) = \mathrm{tr}\,[\exp(-\beta H)]$$
$$\beta = 1/k_B T \tag{2.1}$$

Here H is the Hamiltonian operator for N water molecules, consisting of kinetic (K) and potential (V) energy parts:

$$H = K + V \tag{2.2}$$

The trace in eq 2.1 must be carried out over a suitable complete set of functions of both position and spin variables.

The configuration of any molecule j ($1 \le j \le N$) can be described by a nine-component vector $\mathbf{x}_j$ which specifies center-of-mass position, orientation, and vibrational deformation. The potential energy function $V(\mathbf{x}_1 \ldots \mathbf{x}_N)$ can be assumed to be bounded and at least twice differentiable over the entire $9N$-dimensional configuration space, except for those divergences to plus infinity associated with nuclear coincidences. Quite generally we can suppose that V has the following form:[5]

$$V = \sum_j V^{(1)}(\mathbf{x}_j) + \sum_{j<k} V^{(2)}(\mathbf{x}_j,\mathbf{x}_k) + \sum_{j<k<l} V^{(3)}(\mathbf{x}_j,\mathbf{x}_k,\mathbf{x}_l) + \ldots \tag{2.3}$$

The single-molecule function $V^{(1)}$ includes the intramolecular force field as well as interactions with external potentials (container walls, gravity). Pair interactions have been denoted by $V^{(2)}$ and include the all-important propensity for water molecules to form directional, linear hydrogen bonds. The nonadditivity corrections $V^{(3)}$, $V^{(4)}$, ... are known to play a relatively significant role in water.[6] We will assume for the moment that the water molecules cannot dissociate into H^+ and OH^- ions, or exchange hydrogens.

The "inherent structures" that play a key role in the present development are those system configurations for which all forces vanish, i.e., relative minima in V. When N is of the order of Avogadro's number the totality of these minima is huge. Many are related merely by permutation of identical particles, the number of which is $2^N N!$ in the present case. However, even after accounting for this permutation factor, general arguments[4] lead to the conclusion that the number of essentially distinct minima rises exponentially fast with N. Included among these distinct minima of course is one which yields the absolute mini-

(1) D. Eisenberg and W. Kauzmann, "The Structure and Properties of Water", Oxford University Press, New York, 1969.
(2) F. Franks, Ed., "Water, A Comprehensive Treatise", Vol. 1, Plenum Press, New York, 1972.
(3) F. H. Stillinger and T. A. Weber, *Kinam*, **3A**, 159 (1981).
(4) F. H. Stillinger and T. A. Weber, *Phys. Rev. A*, **25**, 978 (1982).
(5) F. H. Stillinger, *Adv. Chem. Phys.*, **31**, 1 (1975).
(6) P. Schuster, "Energy Surfaces for Hydrogen-Bonded Systems", in "The Hydrogen Bond", Vol. I, P. Schuster, G. Zundel, and C. Sandorfy, Ed., North-Holland, New York, 1976, pp 25–163.

0022-3654/83/2087-2833$01.50/0

mum for V, and this should correspond to the most stable crystalline structure at absolute zero temperature.

We now introduce a mapping M of the system configurations $\mathbf{x} \equiv \mathbf{x}_1, \mathbf{x}_2, \ldots, \mathbf{x}_N$ onto the discrete minima of V, for which α serves as an index:

$$M(\mathbf{x}) = \alpha \tag{2.4}$$

This mapping is simply generated by the steepest descent path on the V hypersurface which begins at $\mathbf{x}$ and converges onto α. These paths can be generated as solutions to the partial differential equation[4]

$$d\mathbf{x}/dt = -\nabla V(\mathbf{x}) \tag{2.5}$$

We note in passing that M is undefined for those $\mathbf{x}$ at "saddle points" in the $9N$-dimensional configuration space, but since these constitute a set of zero measure they can be disregarded for present purposes.

Denote by $R(\alpha)$ the set of configurations which M maps onto α. This set is connected and has the minimum α in its interior. It is the region all of whose points "quench" by eq 2.5 to α. The union of $R(\alpha)$ for all α is the entire configuration space itself.

It is now natural to express Q_N as a sum of contributions from each $R(\alpha)$. For this purpose we first write the trace in eq 2.1 as an integral over $\mathbf{x}$:

$$Q_N(\beta) = (C_N/2^N N!) \int B(\mathbf{x},\beta)\, d\mathbf{x}$$

$$C_N = (2S_H + 1)^{2N}(2S_O + 1)^N \tag{2.6}$$

where S_H and S_O are the spins of the hydrogen and oxygen nuclei present (assumed in each case to be isotopically pure), and where the $9N$-dimensional integration includes all accessible configurations. The function $B(\mathbf{x},\beta)$ appearing in eq 2.6 is an appropriately normalized Slater sum:

$$B(\mathbf{x},\beta) = (2^N N!/C_N) \sum_{n,S} \Psi_n^*(\mathbf{x},S) \exp(-\beta H)\, \Psi_n(\mathbf{x},S) \tag{2.7}$$

In this last expression S stands collectively for all spin variables, and n is an index spanning the entire complete set of spin and space wave functions Ψ_n. The normalization chosen for B is such that in the classical limit

$$B \sim \lambda_H^{-6N} \lambda_O^{-3N} \exp(-\beta V) \tag{2.8}$$

where λ_H and λ_O are the relevant mean thermal deBroglie wavelengths. However, it must be stressed that this formal limit is *not* relevant to ordinary temperatures, where the vibrational normal modes of the molecules remain largely in their ground states.

We can obviously rewrite eq 2.6 in the following way:

$$Q_N(\beta) = (C_N/2^N N!) \sum_\alpha \int_{R(\alpha)} B(\mathbf{x},\beta)\, d\mathbf{x} \tag{2.9}$$

where now the integrations span the separate regions $R(\alpha)$. On account of the symmetry of H under particle permutation B will be identical in those R's which differ only by such permutations. Consequently it is useful to collect all equivalent terms in the α sum in eq 2.9 to yield

$$Q_N(\beta) = C_N \sum_\alpha{}' [\sigma(\alpha)]^{-1} \int_{R(\alpha)} B(\mathbf{x},\beta)\, d\mathbf{x} \tag{2.10}$$

where the primed summation only includes one minimum from each permutational equivalence class. The quantity $\sigma(\alpha)$ is a geometric symmetry factor for structure α; it is the number of equivalent structures (permutations) that can be achieved by rigid-body rotation of the system as a whole that do not require surmounting potential energy barriers.

We will denote by V_α the potential energy at minimum α. Then if within $R(\alpha)$ we set

$$B(\mathbf{x},\beta) = \lambda_H^{-6N} \lambda_O^{-3N} \exp(-\beta V_\alpha) b_\alpha(\mathbf{x},\beta) \tag{2.11}$$

the expression for the partition function becomes

$$Q_N(\beta) = C_N \lambda_H^{-6N} \lambda_O^{-3N} \sum_\alpha{}' [\sigma(\alpha)]^{-1} \exp(-\beta V_\alpha) \int_{R(\alpha)} b_\alpha(\mathbf{x},\beta)\, d\mathbf{x} \tag{2.12}$$

In virtue of eq 2.8, each b_α in the classical limit will equal unity at its corresponding potential energy minimum.

The density of distinct potential energy minima, measured along the potential energy axis on a per-molecule basis, is provided by the function

$$G(u) = \sum_\alpha{}' \delta(u - V_\alpha/N)/\sigma(\alpha) \tag{2.13}$$

When N is large we can expect to have[4]

$$\ln G(u) \sim Ng(u) \tag{2.14}$$

where g is independent of system size. Although the inherent structures that contribute to g in the neighborhood of some physically accessible u can be expected to show diversity, we know that they will be sufficiently large in number that their intensive properties (such as density) will have well-defined averages with small relative deviations from those averages.

In the same spirit we can assume that the "vibrational" integrals for each α in eq 2.12 will have narrowly distributed values for those minima clustered around u. Hence we define the "vibrational" free energy per molecule $f(\beta,u)$ by the expression

$$f(\beta,u) = -\lim_{N\to\infty} (N\beta)^{-1} \ln \left\langle \int_{R(\alpha)} b_\alpha(\mathbf{x},\beta)\, d\mathbf{x} \right\rangle_u \tag{2.15}$$

where the average includes all minima in some infinitesimal interval about u. We can now assemble the eq 2.12–2.15 into the final form:

$$Q_N(\beta) = \lambda_H^{-6N} \lambda_O^{-3N} \int \exp\{N[g(u) - \beta u - \beta f(\beta,u)]\}\, du \tag{2.16}$$

This way of writing the partition function exhibits an explicit separation of the inherent structural aspects of the many-body system (embodied in g), from the vibrational part (expressed by f) arising from quantum zero-point motion and from thermal excitation. It should be stressed that eq 2.16 is exact, subject to the large-system limit invoked in its derivation. Whether or not it is useful for understanding water has yet to be demonstrated.

That the large number N occurs in the exponent of the integrand in eq 2.16 motivates an evaluation by the "maximum term" method. For any given β let $u_m(\beta)$ be that value of the potential energy per molecule for which

$$g(u) - \beta u - \beta f(\beta,u) = \text{absolute maximum} \tag{2.17}$$

Then it follows that

$$\ln Q_N(\beta) \sim N[-\ln(\lambda_H^6 \lambda_O^3) + g(u_m) - \beta u_m - \beta f(\beta,u_m)] \tag{2.18}$$

One of the primary objectives of the present approach is to establish how u_m varies with temperature, and what structural shifts in the corresponding inherent structures this temperature variation implies.

III. Classification of Minima

Some of the mechanically stable structures that a collection of water molecules can adopt are obvious, others are more obscure. We now undertake to survey some of

TABLE I: Densities of Water Molecule Networks

structure	temp, K	density, g/cm^3	ref
ice Ih	273	0.9164	7, p 26
Cl_2 hydrate (class I clathrate)	277	0.7904	8, p 123
class II clathrate (THF + H_2S)	253	0.7844	8, p 130
Br_2 hydrate	263	0.7446	8, p 134
$(CH_3)_3CNH_2$ hydrate	243	0.7012	9
ice Ic	143	0.934	1, p 91
ice III	83	1.14	7, p 64
ice VI	98	1.31	7, p 68
ice VIII	100	1.491	10

the possibilities with a view to understanding their implications for the partition function representation derived in the previous section II. To keep the analysis as simple as possible attention will be confined to zero-pressure structures, so we can suppose that the molecules at the minima will be clustered away from contact with container walls.

Table I lists some of the known water molecule networks that exist in the ices and in the clathrate hydrate networks, giving for each the mass density. Of course these are a very special class of structures, but they serve to illustrate the important point that the range of achievable densities spans at least a factor of 2. In the cited cases of high-pressure ice structures the materials typically were quenched to very low temperature to assure kinetic stability before pressure was reduced. Strictly speaking the positive temperature results in Table I should be corrected for thermal expansion and referred to 0 K; however, such corrections are expected to be small and not to affect substantially the considerable spread in relative densities.

Hexagonal ice is the most familiar entry in Table I. Because of the proton disorder present in this crystal[11,12] many inequivalent molecular arrangements are actually comprised in this entry, numbering roughly $(3/2)^N$. No doubt there is some energy spread over this group of Bernal–Fowler–Pauling structures, but that spread is thought to be small. The average binding energy within this group of states is 11.3 kcal/mol for H_2O,[13] from which it can be inferred (by subtraction of zero-point energy) that the mean value for the corresponding collection of potential minima is −13.36 kcal/mol.[14] The zero-pressure structure giving the absolute minimum potential energy presumably is included in this collection, and can be expected to display proton long-range order.

In addition to the multiplicity of minima attributable to proton disorder in perfectly coordinated hexagonal ice, further minima can be expected at some cost in energy as point defects are inserted into the lattice. These include vacancies, interstitials, and Bjerrum orientational defects.[7]

Cubic ice (Ic) has virtually the same density as hexagonal ice (Ih) at the low temperatures where both are kinetically stable. However, there is no reason to suspect that ice Ic is *thermodynamically* more stable than ice Ih at any temperature, including 0 K. While its average is thus in principle higher (and the same is then true for the mean value of the potential minima), cubic ice probably lies very close in energy to hexagonal ice.

The high-density structures formed by quenching and decompressing the high-pressure ices no doubt have relatively high energy, the more so the higher their density. This arises from incorporation of bent hydrogen bonds (ices III and VI) or from repulsive close contacts between molecules not directly hydrogen bonded (ice VIII). Olinger and Halleck[15] have estimated the lattice energy differences between ice Ih and ice VIII extrapolated to 298 K and zero pressure to be 1.08 kcal/mol; this is unlikely to change much by cooling to 0 K.

The clathrate frameworks manage to achieve low density by incorporating several types of face-sharing polyhedral cavities.[16] These are geometrically possible while the network still maintains the natural tendency for each water molecule to engage in exactly four linear hydrogen bonds at approximately tetrahedral angles. The reduction in density below that of ice Ih evidently entails some loss of cohesive energy, due perhaps to attenuation of London dispersion attractions. Incorporation of guest molecules within these structures clearly makes up for the loss. Barrer and Edge[17] have calculated that on average it takes approximately 0.35 kcal to rearrange 1 mol of ice Ih into the empty class I clathrate structure. In view of the expected similarity of vibrational motions in ice Ih and this clathrate, this number can be taken roughly as the difference in mean values of the corresponding groups of potential minima. The clathrate group presumably exhibits proton disorder of the Bernal–Fowler–Pauling type. Similar but somewhat larger rearrangement energies should be expected for the clathrate networks that have even lower density.

"Mixed" structures are certainly possible. The most obvious case involves ices Ih and Ic because of their nearly identical lattice spacings. Indeed if the former is created by adding successive layers one on the other along the hexagonal c axis, stacking faults of ice Ic type can be interposed ad libitum without violating the geometric necessities of fourfold tetrahedral bonding. If *every* layer were thus faulted this would simply create the Ic structure; but more interesting is the case of coexisting macroscopic regions of hexagonal and of cubic type joined across a fully hydrogen-bonded seam, with a distribution of potential minima interpolating those of the pure phases.

"Mixed" structures possessing side-by-side domains of other pairs of "pure" structures from Table I are also possible. But generally the latter will be incommensurate and so would necessitate many bent and broken hydrogen bonds at domain walls.

Amorphous ice deposits can be formed both by vapor-phase deposition on very cold surfaces[18,19] and by high-pressure injection of liquid water into cryofluids.[20] In comparison with ice Ih these substances surely have relatively high potential energy, and indeed can be induced to rearrange into crystalline ice by warming. Unfortunately no accurate measurements are available either for cohesive energy or for density of these materials.

(7) N. H. Fletcher, "The Chemical Physics of Ice", Cambridge University Press, London, 1970.
(8) F. Franks, Ed., "Water, A Comprehensive Treatise", Vol. 2, Plenum, New York, 1973.
(9) R. K. McMullan, G. A. Jeffrey, and T. H. Jordan, *J. Chem. Phys.*, **47**, 1229 (1967).
(10) P. J. J. Wong and E. Whalley, *J. Chem. Phys.*, **64**, 2359 (1976).
(11) L. Pauling, *J. Am. Chem. Soc.*, **57**, 2680 (1935).
(12) S. W. Peterson and H. A. Levy, *Acta Crystallogr.*, **10**, 70 (1957).
(13) Reference 1, p 101.
(14) Reference 7, p 41.
(15) B. Olinger and P. M. Halleck, *J. Chem. Phys.*, **62**, 94 (1975).
(16) Reference 8, pp 128–46.
(17) R. M. Barrer and A. V. J. Edge, *Proc. R. Soc. London, Ser. A*, **300**, 1 (1967).
(18) E. F. Burton and W. J. Oliver, *Proc. R. Soc., London, Ser. A*, **153**, 166 (1935).
(19) (a) T. C. Sivakumar, S. A. Rice, and M. G. Sceats, *J. Chem. Phys.*, **69**, 3468 (1978). (b) M. S. Bergren, D. Schuh, M. G. Sceats, and S. A. Rice, *ibid.*, **69**, 3477 (1978).
(20) P. Brüggeller and E. Mayer, *Nature (London)*, **288**, 569 (1980); **298**, 715 (1982).

TABLE II: Quenches for 250-Molecule Water Cluster

case	initial temp, K	⟨V/N⟩, kcal/mol initial	⟨V/N⟩, kcal/mol final	$N_H(-3.0)$	$N_H(-3.5)$	$N_H(-4.0)$
A	0	−12.333 108	−12.333 108	443	442	439
B	248.5	−10.440 038	−12.238 845	445	441	435
C	287.4	−9.704 793	−12.046 893	450	447	430
D	300.0	−9.283 039	−11.865 829	454	437	413
E	309.3	−8.850 360	−11.624 627	449	432	416
F	334.1	−8.267 230	−11.384 275	441	425	396
G	356.0	−7.873 481	−11.417 074	437	414	385
H	288.4	−8.982 122	−11.543 295	440	422	402
I	255.4	−9.535 264	−11.725 234	460	435	395
J	259.8	−9.561 646	−11.636 086	447	430	401

A precise definition of "hydrogen bond" between two water molecules is required to classify the wide range of possible inherent structures. We adhere to a definition for which potential energy is basic.[21,22] The general many-molecule interaction shown earlier in eq 2.3 leads to the following quantity for the instantaneous interaction between two molecules j and k:

$$\phi(j,k) = V^{(2)}(\mathbf{x}_j,\mathbf{x}_k) + \tfrac{1}{3}\sum_{l(\neq j,k)} V^{(3)}(\mathbf{x}_j,\mathbf{x}_k,\mathbf{x}_l) + \tfrac{1}{6}\sum_{l<m(\neq j,k)} V^{(4)}(\mathbf{x}_j,\mathbf{x}_k,\mathbf{x}_l,\mathbf{x}_m) + \ldots \quad (3.1)$$

This symmetrically divides each $V^{(n)}$ among the $n(n-1)/2$ participating pairs. Then the existence of a hydrogen bond between j and k is taken to mean simply that $\phi(j,k)$ falls below some preassigned critical value V_{HB}:

$$\phi(j,k) \geq V_{HB}: \text{ no bond}$$

$$\phi(j,k) < V_{HB}: \text{ hydrogen bond} \quad (3.2)$$

Any sensible and useful definition would require the parameter V_{HB} to be negative. In order that at least the ices Ih and Ic and the clathrate frameworks listed in Table I be classified as four-coordinate at each molecule, we must have V_{HB} fall roughly in the range[22]

$$-4 \text{ kcal/mol} \leq V_{HB} \leq -2 \text{ kcal/mol} \quad (3.3)$$

With this completely general criterion in hand, we can now proceed to study the number and spatial arrangement of hydrogen bonds in an arbitrary structure.

IV. Simulation Results

Using the molecular dynamics method of computer simulation, we have recently examined several thermodynamic states for an isolated cluster of 250 water molecules.[23] Interactions between the molecules were approximated by the pairwise-additive ST2 effective interaction,[24] and classical equations of motion for the simulation were solved without invoking a cutoff on interactions. An external potential was present to prevent evaporation and escape of any molecule and to keep the cluster centered near the coordinate origin; however, its perturbing influence on the cluster per se was negligible.

These cluster calculations provide a convenient basis for construction and analysis of inherent structures in water. Configurations were selected from the dynamical sequences at different cluster temperatures and then were numerically "quenched" to local potential energy minima. This quenching was carried out in two stages for the sake of computational efficiency. First, a strong damping was applied to the classical equations of motion to remove most of the kinetic energy, thereby causing the system to settle quickly and without annealing into a rough approximation to the final inherent structure. Second, a conjugate gradient procedure[25] was invoked to adjust the molecular configuration to the precise position of the local minimum. Calculations were carried out on the Murray Hill CRAY-1, requiring about 7 h to complete to a given quench.

Table II provides data on ten quenches. It lists initial ("fictive") temperatures, and potential energies per particle both as averages in the starting state and as precise values in the corresponding quench minimum. It also gives values for $N_H(V_{HB})$, the number of hydrogen bonds in the quenched state, using the definition of hydrogen bonding advocated in section III with three values for the cutoff:

$$V_{HB} = -3.0, -3.5, -4.0 \text{ kcal/mol}$$

The ten cases A–J presented in Table II appear in the order in which they were generated during the molecular dynamics study.[23] Case A is in fact already quenched; it is a mechanically stable arrangement of the 250 water molecules that differs in local structure from a macroscopic ice Ih crystal only because of some surface restructuring. Cases B and C resulted from successive heating stages; stereopictures reveal that they are also predominately ice-Ih-like, but with some surface "melting". Case D (300 K) falls at what we have identified as a bulk melting temperature for the ST2 water model, and the prequenched configuration consists of a thick liquidlike mantle surrounding a still-icy core. Case E is nearly but not quite fully melted, while cases F and G are unambiguously liquid droplets. Subsequent cooling stages yielded the slightly supercooled (for ST2) liquid cluster H and the deeply supercooled clusters I and J. On the time scale available to molecular dynamics computer simulation there is virtually no chance that these last three states would spontaneously nucleate to re-form ice Ih.

Surface effects on a free cluster of 250 molecules are obviously extremely important. Since our primary interest lies in extracting information about bulk water from the cluster calculations some strategy is necessary to neutralize these surface effects. We have elected to identify a set of "cluster-core molecules", namely, those whose centroids lie within 9.0 Å of the coordinate origin (which was always nearly coincident with the centroid of the entire cluster). Because this subset had no exposed surface it seemed reasonable to suppose that its properties on average could approximate those of bulk samples.

Table III indicates the number N_c of cluster-core molecules found for each of the ten configurations A–J, both before and after quenching to the potential minima.

(21) F. H. Stillinger and A. Rahman, *J. Chem. Phys.*, **57**, 1281 (1972).
(22) A. Rahman and F. H. Stillinger, *J. Am. Chem. Soc.*, **95**, 7943 (1973).
(23) T. A. Weber and F. H. Stillinger, *J. Phys. Chem.*, in press.
(24) F. H. Stillinger and A. Rahman, *J. Chem. Phys.*, **60**, 1545 (1974).
(25) R. Fletcher, "Practical Methods of Optimization", Wiley, New York, 1980.

TABLE III: Properties of the Cluster-Core Subsets

case	initial temp, K	initial configuration N_c	initial configuration V_c/N_c, kcal/mol	quenched configuration N_c	quenched configuration V_c/N_c, kcal/mol
A	0	92	−14.324 078	92	−14.324 078
B	248.5	94	−12.395 299	95	−14.157 279
C	287.4	92	−11.301 383	96	−13.542 428
D	300.0	88	−10.006 739	93	−12.774 206
E	309.3	87	−9.254 8781	84	−12.291 183
F	334.1	73	−8.715 0564	89	−12.001 963
G	356.0	74	−8.758 1757	82	−12.232 628
H	288.4	96	−9.795 7042	98	−12.214 847
I	255.4	85	−10.336 641	106	−12.609 166
J	259.8	82	−10.116 076	90	−12.303 017

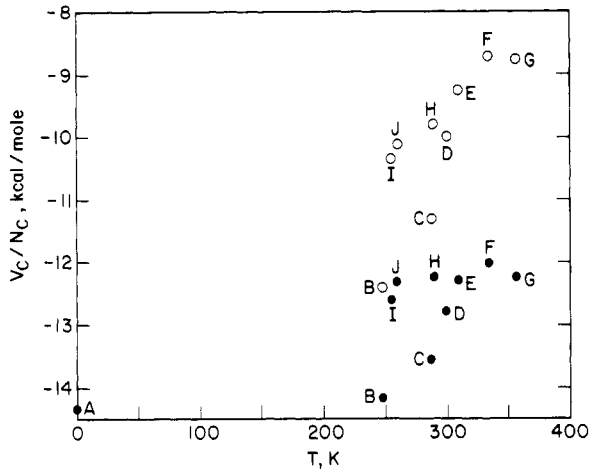

Figure 1. Cluster-core potential energy per particle before (open circles) and after (filled circles) quenching.

Changes in these integers reflect the *relaxation processes* at work during the quenching, but in any case N_c remains around 90.

The potential energy V_c of the cluster-core molecules consists partly of pair interactions within this subset, and partly of pair interactions with the surrounding layer of cluster-surface molecules. The latter must be symmetrically split between core and surface subsets. Thus we set

$$V_c = \sum_{i<j=1}^{N_c} V^{(2)}(i,j) + \tfrac{1}{2}\sum_{i=1}^{N_c}\sum_{j=N_c+1}^{N} V^{(2)}(i,j) \qquad (4.1)$$

where the serial numbering first exhausts the core subset, and where $N = 250$ for the present simulation. Values of V_c/N_c before and after quenching for the ten cases are provided both in Table III and in Figure 1.

Our V_c/N_c information is very sparse and should not be overinterpreted. Nevertheless some interesting qualitative conclusions seem to be suggested. It is useful to examine linear least-squares fits to the values determined for the five liquid-state cases F, G, H, I, and J. Such a fit may be a reasonable estimate of the average of many such initial-configuration selections and their quenching endpoints. Before quenching, the result is (in kcal/mol)

$$\langle V_c/N_c\rangle \simeq 0.01663T - 14.5124 \qquad (4.2)$$

while after quenching

$$\langle V_c/N_c\rangle_q \simeq 0.003366T - 13.2779 \qquad (4.3)$$

These fitting functions must not be taken too seriously at very low temperature. In particular the former extrapolates at $T = 0$ to a potential energy *below* that of the perfect crystal, an obvious absurdity. Also the two linear curves cross at $T = 93.1$ K, which is impossible. But between roughly 250 and 360 K they should provide qualitatively useful guides.

If the vibrational excitations removed by the quenching were strictly harmonic, then the familiar classical equipartition principle would require

$$(d/dT)(\langle V_c/N_c\rangle - \langle N_c/N_c\rangle_q) = 3k_B = 0.005693 \text{ kcal/(mol K)} \qquad (4.4)$$

That the actual slope difference implied by eq 4.2 and 4.3 is substantially larger

$$(d/dT)(\langle V_c/N_c\rangle - \langle V_c/N_c\rangle_q) = 0.013264 \text{ kcal/(mol K)} \qquad (4.5)$$

reveals strong anharmonicity. Restoring forces present in the liquid phase thus tend to be weaker than harmonic. Put another way, the potential energy hypersurface tends to flatten out substantially along many directions at those elevations above the minima which are probed thermally in the liquid state. In line with Rahman's observations for molecular dynamics simulations of monoatomic liquids,[26] one should expect that unquenched configurations for liquid water would show dynamical motions characterized by many imaginary frequencies (negative curvature directions in V).

Vibrational excitation energy is found to be greater than that for harmonic motion over the entire 250–360 K range. On account of the large slope difference noted above the discrepancy is diminished substantially toward the low temperature end. In part this may be due simply to diminished vibrational amplitude. But the effect is so large that likely the inherent structures applicable at the lower temperatures are manifestly more harmonic (structurally tighter) than those generated by quenching from higher temperature.

Comparison between cases C and H is suggestive in regards to the source of the latent heat of melting (experimentally equal to 1.44 kcal/mol at 273.2 K). They both have nearly the same starting temperature which is only slightly below the apparent melting point for the ST2 model. The former (C) has a cluster core that is substantially unmelted, while the latter (H) is liquid throughout. The difference in potential energy per particle before quenching is 1.51 kcal/mol while after quenching it drops only slightly to 1.33 kcal/mol. If these numbers are typical, then about 88% of the latent heat must be ascribed to the upward shift in position of contributing minima along the potential energy scale, while the remaining 12% arises from increasing anharmonicity of vibrations in passing from crystalline to amorphous structures.

This last result stands in significant contrast to melting of simple substances in two dimensions. In particular we can cite a dynamical and quenching study of the Gaussian core model in two dimensions[3,4] which shows that only about one-quarter of the latent heat is attributable to upward shift in minima, three-quarters to increasing anharmonicity.

Figure 2 shows how cluster-core molecules in the quenches A, C, and H are distributed according to hydrogen bond number n_H. The cutoff V_{HB} was set at −3.5 kcal/mol for these histograms. Not surprisingly, all core molecules in the ice crystallite A engage in exactly four hydrogen bonds. Case C shows some deviation from this ideal even though its core is still obviously crystalline upon examination of stereophotographs. The 3-fold and 5-fold coordinations arise from the surface melting that has taken

(26) A. Rahman, unpublished results.

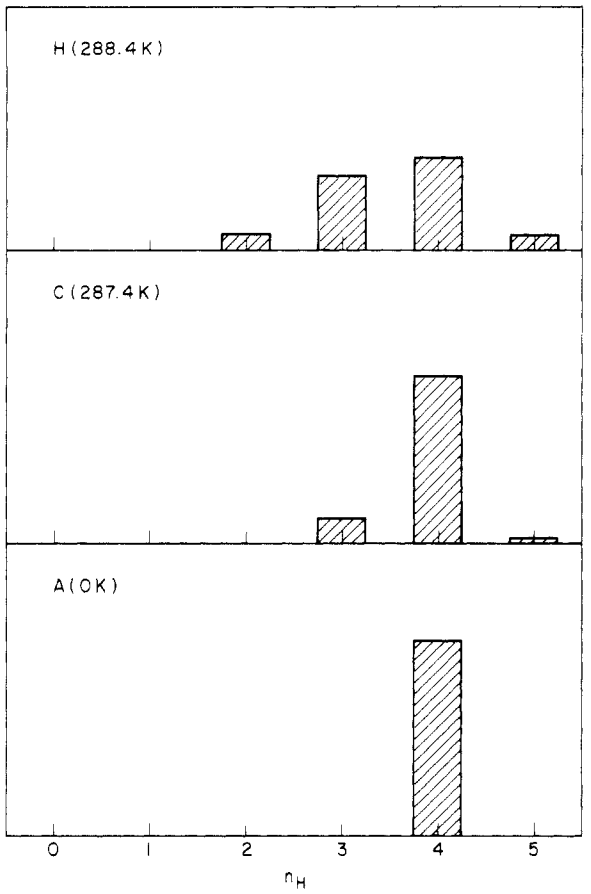

Figure 2. Distributions of cluster-core molecules according to the numbers n_H of hydrogen bonds in which they engage. $V_{HB} = -3.5$ kcal/mol. The cases shown are quenches from configurations A, C, and H (see Tables II and III); the first two are icelike, the last is amorphous.

place; some core molecules reside next to displaced mantle molecules. Comparison of histograms for C and H show how melting implies profound changes in the hydrogen bond statistics of the corresponding inherent structures. Not only does melting cause a reduction in the mean number of hydrogen bonds, but the breadth of the distribution increases.

V. Water Anomalies

The liquid-phase density maximum at $T_{max} = 4$ °C is the most prominent and widely publicized of the water anomalies. It is the low-pressure manifestation of a more extensive anomaly: A locus of density-maximum temperatures $T_{max}(p)$ exists even at somewhat elevated pressure p, though increasing p causes T_{max} to decline and eventually to disappear.[27] It is natural now to consider how this phenomenon can arise in the present inherent structure context.

At any fixed pressure the molar volume v_0 of water can be written as the sum of two contributions:

$$v_0(T,p) = v_q(T,p) + \Delta v_q(T,p) \tag{5.1}$$

Here v_q stands for the mean molar volume of the quenched states that originated in the water at T,p (where it is understood that quenching occurs at fixed p). Each one of these quenches, while confined to its characteristic region $R(\alpha)$, would manifest some volume change if reheated from absolute zero to the temperature of interest T; Δv_q stands for the mean change in molar volume of these $R(\alpha)$-confined structures upon constant-p reheating. This second contribution would vanish if the thermal excitation were strictly harmonic, but of course it is not. The existence of a density maximum requires

$$[\partial v_q/\partial T]_p = -[\partial \Delta v_q/\partial T]_p \tag{5.2}$$

along the locus $T_{max}(p)$ in the T,p plane.

The coefficient of thermal expansion of ice Ih at 260 K and ambient pressure is[28]

$$(\partial \ln v_0/\partial T)_p = 1.52 \times 10^{-4}\ \text{deg}^{-1} \tag{5.3}$$

and it is increasing somewhat with temperature. We have noted above that ice Ih consists really of a large collection of alternative structures owing to proton disorder. The value in (5.3) is an average for those Bernal–Fowler–Pauling configurations. But since all of those canonical ice structures have the same hydrogen-bond network geometry and nearly the same cohesive energy, none is likely to have its thermal expansion deviate significantly from the mean. Because the empty clathrate networks also display the same tetrahedral hydrogen bond coordination at every water molecule, the thermal expansivity of these other families of structures should also be roughly comparable to the ice value shown in eq 5.3.

Inherent structures that underlie the liquid state surely have imperfect hydrogen bonding and have less cohesive energy than ice. These softer and more anharmonic structures then ought to have thermal expansions that are positive and at least as large as that shown above for ice. At T_{max} such expansion must be cancelled according to eq 5.2 by a reduction in v_q with increasing T, which the above reasoning indicates must have a magnitude

$$[\partial \ln v_q/\partial T]_p \lesssim -1.5 \times 10^{-4}\ \text{deg}^{-1} \tag{5.4}$$

at least in the low pressure regime. This reaffirms the conventional wisdom that bulky structures are important for water at low temperature, while more compact structures predominate at higher temperature. Now, however, the term "structure" has been given a precise meaning, namely, the relevant set of quenches.

Because T_{max} at 1 atm is so close to the melting point temperature T_m it is reasonable to suppose that temperature derivatives of v_q and Δv_q continue to have the same signs and magnitudes down to, and below, T_m. Of course the exact balance shown in eq 5.2 is now upset: As T decreases below T_{max} the negative quantity $(\partial v_q/\partial T)_p$ dominates the positive quantity $(\partial \Delta v_q/\partial T)_p$ more and more.

One of the fascinating attributes of the deeply supercooled regime is that $(\partial v_0/\partial T)_p$ as well as many other physical properties appear to be headed for infinite singularities of algebraic character at a common temperature T_s equal to 228 K.[29] Symbolically, property X behaves thus

$$X(T) \sim A_X(T - T_s)^{-\gamma} \tag{5.5}$$

where A_X is a constant and exponent γ controls the rate of divergence. For $(\partial v_0/\partial T)_p$ the exponent γ is approximately 0.98, while for isothermal compressibility and constant-pressure heat capacity it is approximately 0.35.[29]

In order to discuss supercooling anomalies adequately we need to return to the partition function representation shown earlier in eq 2.16, with one important modification. To confine attention to the supercooled state we must project out of consideration all inherent structures which

(27) Reference 1, p 185; ses also H. Kanno and C. A. Angell, *J. Chem. Phys.*, **73**, 1940 (1980).

(28) Reference 1, p 104.

(29) R. J. Speedy and C. A. Angell, *J. Chem. Phys.*, **65**, 854 (1976).

consist wholly or in substantial part of crystalline arrangements of molecules. This projection operation has the effect of modifying the density of states function for minima $g(u)$ to another function $g_a(u)$ appropriate for the amorphous subset of structures. Obviously

$$g_a(u) \leq g(u) \tag{5.6}$$

Similarly we must replace the vibrational free energy function $f(\beta,u)$ with $f_a(\beta,u)$ for the amorphous subset. Owing to greater softness and anharmonicity of the amorphous structures compared to their crystalline counterparts, it is a reasonable expectation that

$$f_a(\beta,u) \leq f(\beta,u) \tag{5.7}$$

It is important to consider for the moment what the postulated projection is required to do. It must exercise pattern recognition capacity to exclude inherent structures which contain crystalline regions larger in all dimensions than some preassigned diameter. Not only must regions of ice Ih character be excluded, but so too must *any* periodic array of oxygens such as that in ice Ic and those in the empty clathrate frameworks. The latter become important because estimates have been made[30] indicating that they become thermodynamically more stable than supercooled water below about −25 °C.

The maximal crystal fragment that is allowable before an inherent structure must be rejected is somewhat arbitrary, a feature which should not lightly be dimissed. On the one hand, the critical crystallite diameter cannot be allowed to be as large as 1 μm since this would admit structures that conventionally would be classified as polycrystalline. On the other hand, choosing the critical diameter as small as 5 Å would be so restrictive that it would inhibit structural fluctuations that are a natural and frequent occurrence in liquid water even at room temperature. Presumably there is a compromise choice, probably lying in the 10–30-Å range, which excludes polycrystalline configurations while leading to predictions of liquid water properties into the moderately supercooled regime that are sensibly independent of that choice.

Our use of the projection operation for theoretical study of the supercooled liquid parallels laboratory practice. In both instances it is mandatory to avoid occurrence of critical nuclei of the crystal within the liquid medium around which the solid phase would immediately grow.

The amorphous-structure-projected version of eq 2.18 is as follows:

$$\ln Q_N^{(a)}(\beta) \sim N[-\ln(\lambda_H^6\lambda_O^3) + g_a(u_m) - \beta u_m - \beta f_a(\beta,u_m)] \tag{5.8}$$

The quantity u_m of course is now determined by the corresponding modification of eq 2.17:

$$g_a(u) - \beta u - \beta f_a(\beta,u) = \text{absolute maximum} \tag{5.9}$$

A graphical analysis is useful. Figure 3 schematically shows g_a and curves for $-\beta(u + f_a)$ at several representative temperatures. The quantity u_m corresponds to positions at which the two curves for the given temperature have equal but opposite slopes. As temperature declines it is clear that u_m must drift to more negative values representing more and more strongly hydrogen-bonded inherent structures.

The minimum achievable potential energy per molecule for the amorphous subset has been denoted by u_0 in Figure 3. In principle it depends on the critical crystallite diameter of the projection operation. This minimum will be attained in structures which take maximum advantage of tetrahedral bonding opportunities at each water molecule, while not doing so in a way which incorporates large periodic domains.

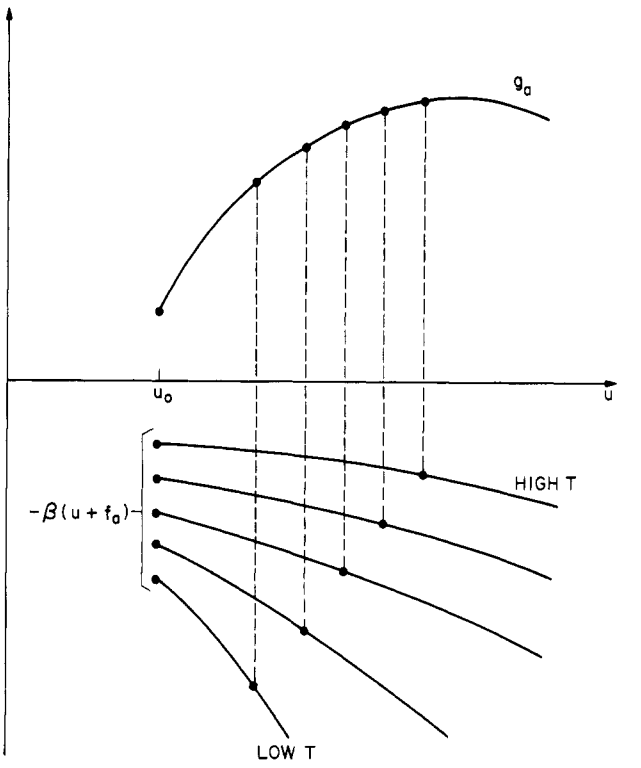

Figure 3. Schematic representation of the evaluation of free energy for the normal and supercooled liquids via eq 5.6.

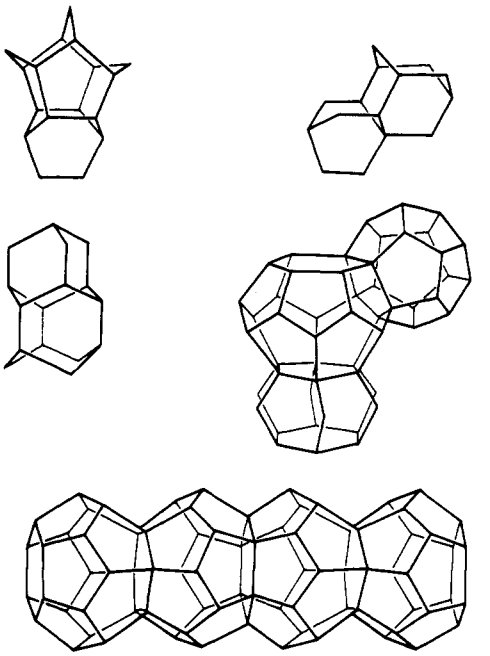

Figure 4. Face-sharing polyhedra that can be incorporated within extended random structures. Vertices represent positions of oxygen atoms, and edges symbolize hydrogen-bonded nearest neighbors.

It has been pointed out before[31,32] that one way to attain strong hydrogen bonding in random networks of water without crystallites is to utilize a random agglomeration of face-sharing polyhedra. Some of the many structural

(30) R. J. Speedy, private communication.

(31) F. H. Stillinger, *Science*, **209**, 451 (1980).

(32) F. H. Stillinger in "Water in Polymers", S. P. Rowland, Ed., American Chemical Society, Washington, DC, 1980, ACS Symp. Ser. No. 127, pp 11–21.

possibilities are illustrated in Figure 4. Two features deserve attention. First, the number of distinct feasible polyhedra is quite large; they include but are not restricted to ice Ih and Ic polyhedra. Second, they tend in an important sense to be "autocatalytic"; the presence of one well-formed polyhedron in the matrix predisposes toward the existence of another because the molecules on any given face are already properly positioned to act as a template for completion of the partner sharing that face. Amorphous inherent structures will be forced to use this architectural ploy more and more frequently as the potential energy per particle declines. Upon close approach to the lower limit u_0 it seems inevitable that the number of face-sharing polyhedra would suddenly rise, forming in fact a macroscopically connected mass. Because the majority of the available polydedra are so bulky, the mean molar volume v_q of the quenched structures should rise in a singular manner, though possessing a well-defined limiting value.

It is a straightforward matter to see how supercooling singularities at T_s *might* arise from eq 5.8, and being aware of such possibilities could be useful in guiding future studies. In particular suppose that near u_0 the density of states g_a has the following expansion:

$$g_a(u) = g_a(u_0) + a_1(u - u_0) - a_2(u - u_0)^p + \ldots \quad (5.10)$$

where a_1 and a_2 are positive constants and exponent p exceeds 1. Furthermore suppose that when u is again close to u_0 and $\beta = (k_B T)^{-1}$ is close to the singularity value $\beta_s = (k_B T_s)^{-1}$

$$u + f_a = b_0 + b_1(u - u_0) + \ldots \quad (5.11)$$

b_0 and b_1 are constants, the latter one positive. Criterion (5.9) can then be implemented to yield

$$\beta_s = a_1/b_1$$

$$u_m(\beta) = [b_1(\beta_s - \beta)/pa_2]^{1/(p-1)} + \ldots \quad (5.12)$$

To be consistent with the previously cited divergence in the constant-pressure heat capacity the exponent in the second of these equations would have to be approximately 1–0.35 = 0.65, which in turn demands that

$$p = 2.54 \quad (5.13)$$

At the present level of precision this is surely indistinguishable from 5/2.

Future effort devoted to the statistical geometry of random networks should help to evaluate the validity of assumptions (5.10) and (5.11).

VI. Summary and Conclusions

The principle concepts presented above may be summarised as follows.

(1) In considering the static properties of water by means of the canonical partition function, there exists a natural and unique separation of the effects of molecular packing geometry on the one hand, from the effects of "vibrational" excitation on the other hand. The former comprise all mechanically stable arrangements of molecules (i.e., relative potential minima), and constitute inherent structures different subsets of which are relevant at different temperatures.

(2) For liquid water near its normal melting point, the mean molar volume of the relevant subsets of inherent structures is less than that of the liquid itself, and is declining with increasing temperature. The density maximum phenomenon represents a balance point between this shrinkage of the relevant inherent structures and the thermal expansion of all structures individually.

(3) Roughly 85–90% of the latent heat of melting ice is attributable to potential energy increase for the inherent structures involved (crystalline below T_m, amorphous above). The remainder is associated with increasing vibrational anharmonicity as the inherent structures change character across the transition.

(4) Supercooling anomalies are associated with incorporation of edge and face sharing polyhedra that appear in the inherent structures with increasing probability as temperature declines. Since these geometric units tend to be bulky and to be "autocatalytic", they cause the relevant inherent structures to decrease dramatically in density and in potential energy as the supercooling limit is approached. Furthermore, their appearance is discouraged by elevating the pressure.

The "inherent structure" view of the various states of water seems to provide a significant conceptual unification. However, the story is far from complete. It is desirable to obtain more information about amorphous water structures both from direct experimental study and from more extensive computer simulations with configurational quenchings. In particular more simulation data of the type shown in Figure 1 would be extremely useful, starting with well-equilibrated samples of strongly supercooled water. It would also be valuable to see how elevated pressure shifts the hydrogen-bonding character of the quenches.

Although attention here has been focussed on pure water, aqueous solutions deserve study as well. It has been suggested[31] that nonpolar (hydrophobic) solutes become encapsulated in convex cages similar to those spontaneously formed in cold pure water, and specifically that they are driven together by the tendency of those cages to share edges and faces (hence explaining hydrophobic attraction). If this suggestion has merit, quenches of the solutions should show the solvation cages in vivid form. At the other extreme, dissolved ions would doubtless produce very different local order in the corresponding electrolytic solution quenches.

Another fascinating aspect of water chemistry concerns dissociation to produce solvated H^+ and OH^- ions. This phenomenon has been specifically excluded in the present study for simplicity, in spite of its obvious importance. Since models for water have begun to emerge in which dissociation is possible[33-35] we conclude that the inherent structure theory should be reexamined in that context. It would be illuminating to see how quenching reduces the extent of dissociation, i.e., causes spontaneous recombination to occur along hydrogen bond pathways.

Registry No. Water, 7732-18-5.

(33) F. H. Stillinger and C. W. David, *J. Chem. Phys.*, **69**, 1473 (1978).
(34) T. A. Weber and F. H. Stillinger, *J. Phys. Chem.*, **88**, 1314 (1982).
(35) T. A. Weber and F. H. Stillinger, *Chem. Phys. Lett.*, **89**, 154 (1982).